Rational Design of a Novel Intercalation System. Layer-Gap Control of Crystalline Coordination Polymers, $\{[Cu(CA)(H_2O)_m](G)\}_n$ ($m = 2$, G = 2,5-Dimethylpyrazine and Phenazine; $m = 1$, G = 1,2,3,4,6,7,8,9-Octahydrophenazine)

Satoshi Kawata, Susumu Kitagawa,* Hitoshi Kumagai, Chihiro Kudo, Hiroe Kamesaki, Tetsuya Ishiyama, Rieko Suzuki, Mitsuru Kondo, and Motomi Katada

Department of Chemistry, Faculty of Science, Tokyo Metropolitan University, Hachioji, Tokyo 192-03, Japan

Received April 1, 1996[⊗]

New copper(II) intercalation compounds, $\{[Cu(CA)(H_2O)_2](G)\}_n$ (H_2CA = chloranilic acid; G = 2,5-dimethylpyrazine (dmpyz) (**1a** and **1b**) and phenazine (phz) (**2**)) have been synthesized and characterized. **1a** crystallizes in the triclinic space group $P\bar{1}$, with $a = 8.028(2)$ Å, $b = 10.269(1)$ Å, $c = 4.780(2)$ Å, $\alpha = 93.85(3)°$, $\beta = 101.01(2)°$, $\gamma = 90.04(3)°$, and $Z = 1$. **1b** crystallizes in the triclinic space group $P\bar{1}$, with $a = 8.010(1)$ Å, $b = 10.117(1)$ Å, $c = 5.162(1)$ Å, $\alpha = 94.40(1)°$, $\beta = 97.49(1)°$, $\gamma = 112.64(1)°$, and $Z = 1$. **2** crystallizes in the triclinic space group $P\bar{1}$, with $a = 8.071(1)$ Å, $b = 11.266(1)$ Å, $c = 4.991(1)$ Å, $\alpha = 97.80(1)°$, $\beta = 99.58(1)°$, $\gamma = 83.02(1)°$, and $Z = 1$. For all the compounds, the crystal structures consist of one dimensional $[Cu(CA)(H_2O)_2]_m$ chains and uncoordinated guest molecules (G). Each copper atom for **1a**, **1b**, and **2** displays a six-coordinate geometry with the two *bis*-chelating CA^{2-} anions and water molecules, providing an infinite, nearly coplanar linear chains running along the *a*-direction. Theses chains are linked by hydrogen bonds between the coordinated water and the oxygen atoms of CA^{2-} on the adjacent chain, forming extended layers, which spread out along the *ac*-plane. The guest molecules are intercalated in between the $\{[Cu(CA)(H_2O)_2]_k\}_l$ layers, just like pillars, which are supported with N···H_2O hydrogen bonding. The guest molecules are stacked each other with an interplanar distance of ca. 3.2 Å along the *c*-axis perpendicular to the $[Cu(CA)(H_2O)_2]_m$ chain. The EHMO band calculations of intercalated dmpyz and phz columns show an appreciable band dispersion of phz π (b_{2g} and b_{3g}) and dmpyz π (b_g), indicative of the importance of planar π structure for the formation of the intercalated structure. The distances of O−H---N (guest molecules) fall within the range 2.74−2.80 Å, insensitive to the guest, whereas the interlayer distances increase in the order 9.25 Å (**1b**), 10.24 Å (**1a**), and 11.03 Å (**2**). The degree in lengthening the distance correlates well with the size of a molecule, indicative of the stability of the 2-D sheet structure and the flexibility of the sheet packing. The magnetic susceptibilities were measured from 2 to 300 K and analyzed by a one-dimensional Heisenberg-exchange model to yield $J = -1.83$ cm^{-1}, $g = 2.18$ (**1a**), $J = -0.39$ cm^{-1}, $g = 2.14$ (**1b**), and $J = -1.84$ cm^{-1}, $g = 2.18$ (**2**). The absolute value of J is smaller than that value for $[Cu(CA)]_n$, which has a planar ribbon structure suggesting that the magnetic orbital $d_{x^2-y^2}$ is not parallel to the chloranilate plane. For comparison with phz another type of copper(II) coordination compound, $\{[Cu(CA)(H_2O)](ohphz)\}_n$ (ohphz = 1,2,3,4,6,7,8,9-octahydrophenazine (**7**)) has also been obtained. **7** crystallizes in the orthorhombic space group *Cmcm* with $a = 7.601(2)$ Å, $b = 13.884(2)$ Å, $c = 17.676(4)$ Å, and $Z = 4$. Nonplanar ohphz molecules are in between $[Cu(CA)(H_2O)_2]_m$ chains with the N···H_2O hydrogen bonding in a fashion parallel to the chain direction. The copper atom shows a five-coordinate square-pyramidal configuration with two CA and one water molecule, thus affording no hydrogen bonding links between chains, dissimilar to **1a**, **1b**, and **2**. The magnetic susceptibilities yield $J = -10.93$ cm^{-1} and $g = 2.00$, comparable to that of the four-coordinate $[Cu(CA)]_n$. On this basis both hydrogen bonding and stack capability of a guest molecule is responsible for building the unique intercalated structure such as is seen in **1a**, **1b**, and **2**.

Introduction

Building transition metal complex-based layers is an important step to create not only a system to perform the optical, electronic, and magnetic functions,[1−12] but also an intercalation system for ion- or molecule-exchange, absorption, and catalytic properties. In order to construct a spatially and electronically well-linked framework a crystalline coordination polymer is the most useful in various assembled systems of copper. However, this synthetic inorganic chemistry has lagged behind the organic chemistry primarily because of the unavailability of suitable

[⊗] Abstract published in *Advance ACS Abstracts,* July 1, 1996.

(1) Nagaoka, Y. *Phys. Rev.* **1966**, *147*, 392.
(2) *Organic and Inorganic Low Dimensional Crystalline Materials*; Delhaes, P.; Drillon, M., Ed.; D. Reidel: Dordrecht, The Netherlands, 1987.
(3) *Magnetic Molecular Materials*; Gatteschi, D.; Kahn, O.; Miller, J. S.; Palacio, F., Ed.; D. Reidel: Dordrecht, The Netherlands, 1991; p 198.
(4) *Inorganic Materials*; Bruce, D. W.; O'Hare, D., Ed.; John Wiley & Sons: New York, 1992.
(5) Borrás-Almenar, J. J.; Coronado, E.; Gómez-Garcia, C. J.; Ouahab, L. *Angew. Chem., Int. Ed. Engl.* **1993**, *32*, 561.
(6) De Munno, G.; Ruiz, R.; Lloret, F.; Faus, J.; Sessoli, R.; Julve, M. *Inorg. Chem.* **1995**, *34*, 408.
(7) De Munno, G.; Julve, M.; Nicoló, F.; Lloret, F.; Faus, J.; Ruiz, R.; Sinn, E. *Angew. Chem., Int. Ed. Engl.* **1993**, *32*, 613.
(8) De Munno, G.; Viterbo, D.; Caneschi, A.; Lloret, F.; Julve, M. *Inorg. Chem.* **1994**, *33*, 1585.
(9) Julve, M.; De Munno, G.; Bruno, G.; Verdaguer, M. *Inorg.Chem.* **1988**, *27*, 3160.
(10) Otieno, T.; Rettig, S. J.; Thompson, R. C.; Trotter, J. *Inorg.Chem.* **1993**, *32*, 1607.
(11) Chen, Z. N.; Fu, D. G.; Yu, K. B.; Tang, W. X. *J. Chem. Soc., Dalton Trans.* **1994**, 1917.
(12) Chen, Z. N.; Qiu, J.; Wu, Z. K.; Fu, D. G.; Yu, K. B.; Tang, W. X. *J. Chem. Soc., Dalton Trans.* **1994**, 1923.

S0020-1669(96)00352-7 CCC: $12.00

molecular building blocks, difficulties in growing crystals due to insolubility, and poor characterization of polymeric compounds, whose properties vary considerably depending on the molecular weight or degree of polymerization. The products described hitherto were frequently obtained as extremely fine precipitates, ill-defined by structural analyses. Still lacking are reports on the relationship between the polymer and monomer structures and between crystal lattices and polymer structures. Therefore, the rational synthesis of coordination polymers in the single-crystal phase is undeveloped.

Polyoxo carbon compounds such as oxalic acid,[13−16] squaric acid,[17−24] and 2,5-dihydroxy-*p*-benzoquinones and its 3,6-disubstituted derivatives ($H_2(R_2$-DHBQ): R = H or substituent)[25−40] have been used and known as double bidentate ligands and are good candidates to provide transition metal or alkaline earth coordination polymers. Chloranilic acid (H_2CA = $H_2(Cl_2$-DHBQ)), is one of the family, affording one dimensional chains of various metal ions. The corresponding copper(II) 1-D polymer, $[Cu(CA)]_n$, was first prepared and magnetic and structural studies appeared in 1962.[34] However, the X-ray crystallographic structure has never been published since in that time, except that EXAFS and magnetic analyses imply one dimensional-ribbon structures for $[Cu(CA)]_n$ and $[Cu(CA)L_2]_n$, where L is a nitrogen-containing ligand such as amines.[30,36] The background of this chemistry prompts us to utilize CA chains of copper as a building block for high dimensional structures. A useful way is to fabricate 2-D coordination polymers by both 1-D polymers and additional bridging ligands by using the interaction between the chains. Very recently we have succeeded in the synthesis and characterization of a 2-D coordination polymer, $[Cu(CA)(pyz)]_n$ (**3**) (pyz = pyrazine),[41] in which coordination bond is utilized to link monomers (0-D motifs). On the other hand, polymers having a hydrogen-bonding link, $[Cu(CA)(MeOH)_2]_n$ (**4**)[41] and $\{[Cu(CA)(H_2O)_2](H_2O)\}_n$ (**6**),[42−44] have also been synthesized. (See Scheme 1).

The hydrogen bonding used here is relevant to realize higher dimensional metal complex assemblies.[45−48] This interaction is specific and directional and is useful to provide not only structural extended arrays[49−52] but also dynamic properties concerning proton-transfer-mediated electron transfer through the hydrogen bond, which is a way to regulate the electronic properties of solids, intramolecular proton transfer, and thermochromic properties of the crystal forms of several organic molecules, such as *N*-salicylideneanilides.[53−57] Thus, one of the best strategies for the rational synthesis of crystalline coordination polymers is to utilize the hydrogen bonding capability of coordinated ligands in addition to their coordination capability.

There is one other thing that is important for the architecture of functional crystalline coordination polymers. As is well illustrated in **6**, the layers of $[Cu(CA)(H_2O)_2]_k$ are further interlinked by interstitial water molecules in between the layers, forming a 3-D network in the crystal.[43] In other words, the compounds with this layer structure can intercalate small molecules such as water. Two-dimensional intercalation chemistry is widely developed in inorganic compounds having layered structures such as potassium graphites and transition metal chalcogenides,[2,4,58] which are nonstoichiometric with a random distribution of inserted species over a proportion of sites. Intercalation compounds are also in the category of host−guest chemistry related to molecular recognition, which, however, requires stoichiometric insertion of species. Host compounds having layered structures are one of the most important targets for this chemistry. The compound having the layers of $[Cu(CA)(H_2O)_2]_k$ is readily synthesized and could intercalate guest molecules stoichiometrically, indicating the suitability for the requirement. On the basis that hydrogen bonding is the attractive motive force in incorporation of guest molecules, the organic molecules having multihydrogen bonding sites would be intercalated into the compound having the layers of $[Cu(CA)(H_2O)_2]_k$. The establishment of this coordination polymer chemistry leads not only to a new stage of the host−guest

(13) Michalowicz, A.; Girerd, J. J.; Goulon, J. *Inorg. Chem.* **1979**, *18*, 3004.
(14) Girerd, J. J.; Kahn, O.; Verdaguer, M. *Inorg. Chem.* **1980**, *19*, 274.
(15) Gleizes, A.; Maury, F.; Galy, J. *Inorg. Chem.* **1981**, *19*, 2074.
(16) Melnik, M.; Langfelderova, M.; Garay, J.; Gazo, J. *Inorg. Chim. Acta* **1973**, *7*, 669.
(17) West, R.; Niu, H. Y. *J. Am. Chem. Soc.* **1963**, *85*, 2589.
(18) Habenschuss, M.; Gerstein, B. C. *J. Chem. Phys.* **1974**, *61*, 852
(19) Benetó, M.; Soto, L.; G-Lozano, J.; Escrivá, E.; Legros, J.-P.; Dahan, F. *J. Chem. Soc., Dalton Trans.* **1991**, 1057.
(20) van Ooijen, J. A. C.; Reedijk, J.; Spek, A. L. *Inorg. Chem.* **1979**, *18*, 1184.
(21) Frauenhoff, G. R.; Takusagawa, F.; Busch, D. H. *Inorg. Chem.* **1992**, *31*, 4002.
(22) Bernardinelli, G.; Deguenon, D.; Soules, R.; Castan, P. *Can. J. Chem.* **1989**, *67*, 1158.
(23) Robl, C.; Weiss, A. *Z. Naturforsch.* **1986**, *41B*, 1341.
(24) Castro, I.; Faus, J.; Julve, M.; Verdaguer, M.; Monge, A.; G-Puebla, E. *Inorg. Chim. Acta* **1990**, *170*, 251.
(25) Robl, C. *Mater. Res. Bull.* **1987**, *22*, 1483.
(26) Robl, C.; Weiss, A. *Mater. Res. Bull.* **1987**, *22*, 497.
(27) Robl, C.; Weiss, A. *Z. Naturforsch* **1986**, *41*, 1495.
(28) Robl, C.; Kuhs, W. F. *J. Solid State Chem.* **1988**, *74*, 21.
(29) Robl, C.; Kuhs, W. F. *J. Solid State Chem.* **1989**, *79*, 46.
(30) Verdaguer, M.; Michalowicz, A.; Girerd, J. J.; Alberding, N.; Kahn, O. *Inorg. Chem.* **1980**, *19*, 3271.
(31) Wrobleski, J. T.; Brown, D. B. *Inorg. Chem.* **1979**, *18*, 498.
(32) Wrobleski, J. T.; Brown, D. B. *Inorg. Chem.* **1979**, *18*, 2738.
(33) Kanda, S. *Bull. Chem. Soc. Jpn., Pure Chem. Sect.* **1960**, *81*, 1347.
(34) Kanda, S. *Bull. Chem. Soc. Jpn., Pure Chem. Sect.* **1962**, *83*, 282.
(35) Kobayashi, H.; Haseda, T.; Kanda, E. *J. Phys. Soc. Jpn.* **1963**, *18*, 349.
(36) Bottei, R. S.; Greene, D. L. *J. Inorg. Nucl. Chem.* **1968**, *30*, 1469.
(37) Coble, H. D.; Holtzclaw, J. H. F. *J. Inorg. Nucl. Chem.* **1974**, *36*, 1049.
(38) Sartene, R.; Boutron, F. H. *Mol. Phys.* **1970**, *18*, 825.
(39) Riley, P. E.; Haddad, S. F.; Raymond, K. N. *Inorg. Chem.* **1983**, *22*, 3090.
(40) Pierpont, C. G.; Francesconi, L. C.; Hendrickson, D. N. *Inorg. Chem.* **1977**, *16*, 2367.
(41) Kawata, S.; Kitagawa, S.; Kondo, M.; Furuchi, I.; Munakata, M. *Angew. Chem., Int. Ed. Engl.* **1994**, *33*, 1759.
(42) Cueto, S.; Straumann, H.-P.; Rys, P.; Petter, W.; Gramlich, V.; Rys, F. *Acta Crystallogr., Sect. C* **1992**, *48*, 458.
(43) Kawata, S.; Kitagawa, S.; Kondo, M.; Katada, M. *Synth. Met.* **1995**, *71*, 1917.
(44) Kawata, S.; Kitagawa, S.; Furuchi, I.; Kudo, C.; Kamesaki, H.; Kondo, M.; Katada, M.; Munakata, M. *Mol. Cryst. Liq. Cryst.* **1995**, *274*, 179.
(45) Robl, C.; Kuhs, W. *J. Solid State Chem.* **1988**, *75*, 15.
(46) Robl, C.; Hentschel, S.; McIntyre, G. *J. Solid State Chem.* **1992**, *96*, 318.
(47) Breeze, S. R.; Wang, S. *Inorg. Chem.* **1993**, *32*, 5981.
(48) Kawata, S.; Kitagawa, S.; Machida, H.; Nakamoto, T.; Kondo, M.; Katada, M.; Kikuchi, K.; Ikemoto, I. *Inorg. Chim. Acta* **1994**, *229*, 211.
(49) Zeegers-Huyskens, T.; Huyskens, P. L. In *Intermolecular Forces-An Introduction to Modern Methods and Results*; Huyskens, P. L., Luck, A. P., Zeegers-Huyskens, T., Eds.; 1991.
(50) Aakeröy, C. B.; Seddon, K. R. *Chem. Soc. Rev.* **1993**, 397.
(51) MacDonald, J. C.; Whitesides, G. M. *Chem. Rev.* **1994**, *94*, 2383.
(52) Bock, H.; Seitz, W.; Havlas, Z.; Bats, J. W. *Angew. Chem., Int. Ed. Engl.* **1993**, *32*, 411.
(53) Mitani, T. *Mol. Cryst. Liq. Cryst.* **1989**, *171*, 343.
(54) Inabe, T.; Okinawa, K.; Okamoto, H.; Mitani, T.; Murayama, Y.; Takeda, S. *Mol. Cryst. Liq. Cryst.* **1992**, *216*, 229.
(55) Nakasuji, K.; Sugiura, K.; Kitagawa, T.; Toyoda, J.; Okamoto, H.; Okinawa, K.; Mitani, T.; Yamamoto, H.; Murata, I.; Kawamoto, A.; Tanaka, J. *J. Am. Chem. Soc.* **1991**, *113*, 1862.
(56) Yang, Q. C.; Richardson, M. F.; Dunitz, J. D. *J. Am. Chem. Soc.* **1985**, *107*, 5535.
(57) Reetz, M. T.; Höoger, S.; Harm, K. *Angew. Chem., Int. Ed. Engl.* **1994**, *33*, 181.
(58) *Intercalation Chemistry*; Whittingham, M. S.; Jacobson, A. J., Ed.; Academic Press: New York, 1982.

Scheme 1

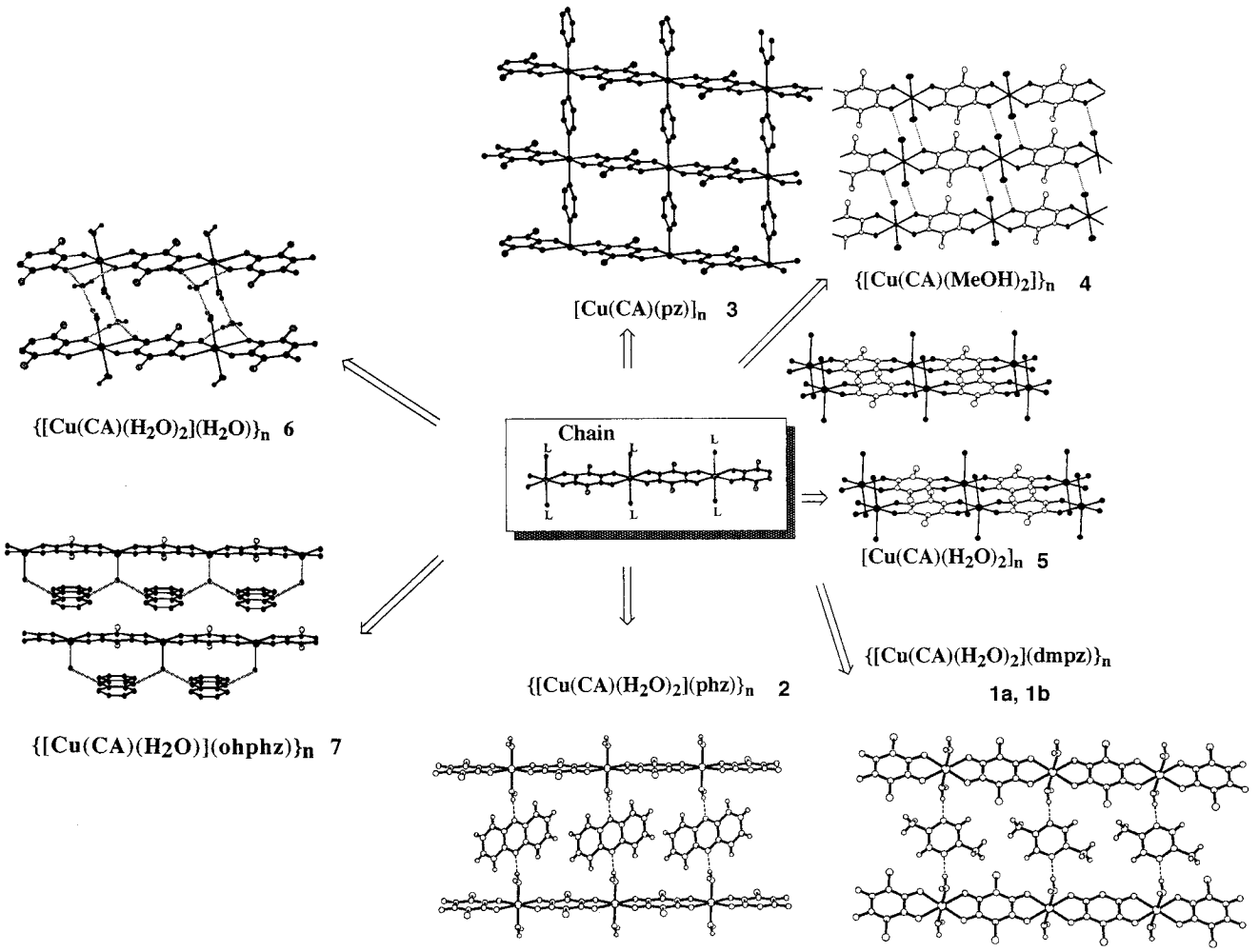

chemistry but also creation of systems having novel solid state properties when the intercalated molecules have a specific function.

In this manuscript, we have succeeded in growing crystals for four compounds, which have common $\{[Cu(CA)(H_2O)_2]_k\}_l$ layers, and demonstrated that the compounds are so flexible that various size of guest molecules are intercalated in between the layers together with the stack column formed. The relationship between the host structure and the intercalated molecule has been examined for the rational design and synthesis. In addition to the crystal structures magnetic and thermal properties were also investigated.

Experimental Section

Syntheses of Compounds. α-**{[Cu(CA)(H$_2$O)$_2$](dmpyz)}$_n$ (1a).** An aqueous solution (10 mL) of copper nitrate (6×10^{-5} mol) was transferred to a glass tube, then an aqueous solution(10 mL) of dmpyz (6×10^{-5} mol) and H_2CA (6×10^{-5} mol) was poured into the tube without mixing the two solutions. Red-purple plate crystals began to form at ambient temperature in a week. One of these crystals was used for X-ray crystallography. Physical measurements were conducted on the crystalline powder obtained from a different batch that was synthesized as follows: An aqueous solution (10 mL) of H_2CA (6×10^{-5} mol) was added dropwise to a 6×10^{-5} mol amount of copper nitrate and a 6×10^{-5} mol amount of dmpyz dissolved in 20 mL of water at 5 °C. When this mixture was stirred a red-purple powder appeared immediately. Anal. Calcd for $CuCl_2O_6N_2C_{12}H_{12}$: C, 34.93; H, 2.44; N, 6.79. Found: C, 34.96; H, 2.76; N, 6.84. IR (KBr pellet): 3258 m, 2969 m, 1638 w, 1516 vs, 1379 s, 1337 w, 1173 w, 1053 s, 999 w, 883 w, 847 s, 760 w, 615 w, 575 w, 491 w cm^{-1}. Raman: 1384, 1597 cm^{-1}. Identity of the batches for physical measurements and single-crystal data collection was established by comparison of the powder X-ray diffraction patterns (XRD). The XRD pattern of the powdered sample is in good agreement with the simulated pattern reproduced from the F_c values of the calculated crystal structure.

β-**{[Cu(CA)(H$_2$O)$_2$](dmpyz)}$_n$ (1b).** The crystal used for X-ray crystallography was obtained by a procedure similar to that of **1a**, except for the temperature which was set higher (45 °C) than the case of **1a**. The magnetic and other physical measurements were conducted on a crystalline powder obtained from a different batch that was prepared at 45 °C in a manner similar to that used for **1a**. When the reaction mixture was stirred, a brown powder appeared immediately. Anal. Calcd for $CuCl_2O_6N_2C_{12}H_{12}$: C, 34.93; H, 2.44; N, 6.79. Found: C, 34.88; H, 2.60; N, 6.82. IR (KBr pellet): 3308 m, 2973 m, 1624 w, 1514 vs, 1381 s, 1337 w, 1290 w, 1173 w, 1053 s, 997 w, 851 s, 743 w, 612 w, 577 w, 483 w cm^{-1}. Raman: 1384, 1597 cm^{-1}. The identity of the magnetic and X-ray batches has been also confirmed by powder XRD pattern.

{[Cu(CA)(H$_2$O)$_2$](phz)}$_n$ (2). An aqueous solution (10 mL) of copper chloride (6×10^{-5} mol) was transferred to a glass tube, then an ethanol−water mixture (10 mL) of phenazine (phz) (6×10^{-5} mol) and H_2CA (6×10^{-5} mol) was poured into the tube without mixing the two solutions. Pale brown plate crystals began to form in a week. One of these crystals was used for X-ray crystallography. The microcrystalline samples were used for physical measurements. They were synthesized as follows: An aqueous solution (10 mL) of H_2CA (6×10^{-5} mol) was added to a 6×10^{-5} mol amount of copper chloride and a 5×10^{-4} mol amount of phenazine dissolved in a mixture of 10 mL of ethanol and 10 mL of water. When the mixture was stirred, a pale brown powder appeared immediately. Anal. Calcd for $CuCl_2O_6N_2C_{18}H_{12}$: C, 44.42; H, 2.49; N, 5.76. Found: C, 44.29; H, 2.40; N, 5.78. IR (KBr pellet): 3258 m, 3057 w, 1636 w, 1523 vs, 1439 w, 1372 w, 1275 w, 1152 w, 1125 w, 999 w, 849 s, 760 s, 594 w, 578 w

Table 1. Crystallographic Data for $\{[Cu(CA)(H_2O)_2](dmpyz)\}_n$ (**1a**), $\{[Cu(CA)(H_2O)_2](dmpyz)\}_n$ (**1b**), $\{[Cu(CA)(H_2O)_2](phz)\}_n$ (**2**), and $\{[Cu(CA)(H_2O)](ohphz)\}_n$ (**7**)

formula	$C_{12}H_{12}N_2O_6Cl_2Cu$ (**1a**)	$C_{12}H_{12}N_2O_6Cl_2Cu$ (**1b**)	$C_{18}H_{12}N_2O_6Cl_2Cu$ (**2**)	$C_{18}H_{12}N_2O_5Cl_2Cu$ (**7**)
fw	414.69	414.69	486.75	476.80
cell consts				
a, Å	8.028(2)	8.010(1)	8.0712(4)	7.601(2)
b, Å	10.269(3)	10.117(1)	11.266(1)	13.884(2)
c, Å	4.780(2)	5.1621(7)	4.9905(9)	17.676(4)
α, deg	93.85(3)	94.40(1)	97.80(1)	90
β, deg	101.01(2)	97.49(1)	99.58(1)	90
γ, deg	90.04(3)	112.64(1)	83.017(8)	90
V, Å^3	385.9(2)	379.1(1)	441.0(1)	1865.5(6)
space group	$P\bar{1}$ (No. 2)	$P\bar{1}$ (No. 2)	$P\bar{1}$ (No. 2)	*Cmcm* (No. 63)
Z	1	1	1	4
ρ(calcd), Mg/cm^3	1.784	1.816	1.833	1.698
μ(Mo Kα), cm^{-1}	17.92	18.24	49.32	14.91
radiation (*λ*, Å)	Mo Kα (0.710 69)	Mo Kα (0.710 69)	Cu Kα (1.541 78)	Mo Kα (0.710 69)
temp, °C	20	20	20	20
R^a	0.030	0.033	0.027	0.064
$R_w{}^b$	0.023	0.028	0.029	0.053

[a] $R = \sum||F_o| - |F_c||/\sum|F_o|$. [b] $R_w = [(\sum w(|F_o| - |F_c|)^2/\sum wF_o^2)]^{1/2}$.

cm^{-1}. Raman: 1283, 1385, 1411, 1474, 1531, 1598 cm^{-1}. The identity of the magnetic and X-ray batches has been confirmed by XRD pattern.

$\{[Cu(CA)(H_2O)_2](ohphz)\}_n$ (7). An ethanol−water (1:1 v/v) mixed solvent was used. A solution (10 mL) of H_2CA (6×10^{-5} mol) was transferred to a glass tube and then a solution (10 mL) of copper chloride (6×10^{-5} mol) and 1,2,3,4,6,7,8,9-octahydrophenazine (ohphz) (6×10^{-5} mol) were poured into the tube without mixing the two solutions. Green crystals began to form in a week. One of these crystals was used for X-ray crystallography. Anal. Calcd for $CuCl_2O_5N_2C_{18}H_{18}$: C, 45.34; H, 3.81; N, 5.88. Found: C, 45.72; H, 3.94; N, 5.78.

Physical Measurements. IR spectra of the KBr disks were measured on a Hitachi I-5040FT-IR spectrophotometer. UV and visible spectra were measured on a Hitachi U-3500 spectrophotometer. EPR spectra were recorded at X-band frequency with a JEOL RE-3X spectrometer operating at 9.1−9.5 GHz. Resonance frequency was measured on an Anritsu MF76A microwave frequency counter. Magnetic fields were calibrated by an Echo Electronics EFM-2000AX NMR field meter. The EPR spectra were recorded with modulation frequency of 100 kHz and modulation amplitude of 0.5 mT, throughout. Magnetic susceptibility data were recorded over the temperature range from 2 to 300 K at 1 T with a SQUID susceptometer (Quantum Design, San Diego, CA) interfaced with an HP Vectra computer system. All data were corrected for diamagnetism which were calculated from Pascal's table. The TIP was assumed to be 60×10^{-6} cm^3 mol^{-1}. Least-squares fitting of the magnetic susceptibility to approximate equations with Heisenberg Hamiltonian ($H = -2J\mathbf{S}_i\cdot\mathbf{S}_j$) for the antiferromagnetic chain[59] were performed. X-ray powder diffraction data were collected on a MAC Science MXP18 automated diffractometer by using Cu Kα radiation. Thermal gravimetric (TG) analyses was carried out with a Seiko Instruments SSC5200 in a nitrogen atmosphere (heating rate: 5 K/min). Laser Raman spectra were recorded with Ar^+ ion excitation using a Jasco R-600 spectrometer. A 90° scattering geometry was employed.

Crystallographic Data Collection and Refinement of the Structure. For each compound, a suitable crystal was chosen and mounted on glass fibers with epoxy resin. Data collections were carried out on a Rigaku AFC7R. Cell constants and the orientation matrix for intensity data collection for each crystal were based on the setting angles of 25 carefully centered reflections in the ranges $25.7 < 2\theta < 34.2°$, $20.4 < 2\theta < 24.7°$, $61.39 < 2\theta < 79.95°$, and $20.30° < 2\theta < 24.95°$ for **1a**, **1b**, **2**, and **7**, respectively. Crystallographic data are given in Table 1. In the case of **7**, the structures were solved by direct methods (Rigaku TEXSAN crystallographic software package of Molecular Structure Corp.). Full-matrix least-squares refinements were carried out with anisotropic thermal parameters for all non-hydrogen atoms. All the hydrogen atoms for **1a**, **1b**, and **2** were located in the Fourier difference maps and refined isotropically. The hydrogen atoms for **7** were placed in the calculated positions for the atoms of C(5) and O(1) and not refined. Toward the end of the development of the structure, the thermal ellipsoid on C(6) indicated disorder. From the difference Fourier peaks this site was remodeled as the two carbon atoms with site occupancies of 50%. These two carbon atoms were refined isotropically. Atomic coordinates are given in Table 2.

The final cycle of full-matrix least-squares refinement for all compounds was based on N_o and n variable parameters and converged (large parameter shift was σ times its esd) with unweighted agreement factors of $R = \sum||F_o| - |F_c||/\sum|F_o|$, $R_w = [\sum(|F_o| - |F_c|)^2/\sum w|F_o|^2]^{1/2}$ where $w = 4F_o^2/\sigma^2(F_o^2)$.

Molecular Orbital Calculations. The extended Hückel (EH) type one-dimensional band calculations[60] were performed to investigate the degree of dispersion relation of inserted dmpyz and phz in **1a**, **1b**, and **2**. A single value of 1.75 as the Wolfsberg-Helmholz constant is used for all the atomic pairs. The 11 k-points are distributed evenly spaced in the chain at intervals of 0.1 (in units of π/|translational vector|).

Results and Discussion

Crystal Structure of 1a. An ORTEP drawing of the structure around the copper in **1a** with the atom numbering scheme is shown in Figure 1a, where the copper atom sits on the crystallographic inversion center. The selected bond distances and angles with their estimated standard deviations are listed in Table 3. The geometry around the copper atom is a distorted elongated octahedron involving the four oxygen atoms of two CA^{2-} anions and two oxygen atoms from two water molecules. There are three pairs of different Cu−O distances; 2.225(2) Å (Cu−O(1) and Cu−O(1′)), 2.057(2) Å (Cu−O(2), Cu−O(2′)) and 1.959(2) Å (Cu−O(3), Cu−O(3′)). Therefore the environment of the copper atom consists of four short in-plane bonds and two long out-of-plane bonds, giving rise to a "2 + 2 + 2" type of configuration. The asymmetrical coordination of the CA^{2-} dianion is also recognized in the different C−O distances; the C(1)−O(1) distance (1.245(3) Å) similar to those reported for a free chloranilate dianion (1.243(7), 1.253(7) Å),[61] and another distance of C(2)−O(2) (1.270(3) Å) close to that of a *p*-quinone form found in **3** and **5**.[25−27,29,39,41,43,62−65] It is worth noting in Figure 1b that the

(59) Hatfield, W. E. *J. Appl. Phys.* **1981**, *52*, 1985.

(60) Kitagawa, S.; Okubo, T.; Kawata, S.; Kondo, M.; Katada, M.; Kobayashi, H. *Inorg. Chem.* **1995**, *34*, 4790.
(61) Andersen, E. K. *Acta Crystallogr.* **1967**, *22*, 191.
(62) Folgado, J. V.; Ibáñez, R.; Coronado, E.; Beltrán, D.; Saavariault, J. M.; Galy, J. *Inorg. Chem.* **1988**, *27*, 19.
(63) Jeong, W.-Y.; Holwerda, R. A. *Inorg. Chem.* **1988**, *27*, 2571.
(64) Calvo, M. A.; Lanfredi, A. M. M.; Oro, L. A.; Pinillos, M. T.; Tejel, C.; Tiripicchio, A.; Ugozzoli, F. *Inorg. Chem.* **1993**, *32*, 1147.
(65) Tinti, F.; Verdaguer, M.; Kahn, O.; Savariault, J.-M. *Inorg. Chem.* **1987**, *26*, 2380.

Table 2. Positional and Equivalent Isotropic Thermal Parameters

atom	*x*	*y*	*z*	B_{eq}, Å^2
(a) α-{[Cu(CA)(H$_2$O)$_2$](dmpyz)}$_n$ (**1a**)				
Cu	1.0000	0.0000	1.0000	1.74(1)
Cl	1.44023(10)	0.22825(8)	0.5769(2)	2.77(2)
O(1)	1.2385(2)	−0.0927(2)	1.2059(4)	2.42(5)
O(2)	1.1837(2)	0.0972(2)	0.8455(4)	2.19(5)
O(3)	1.0074(3)	0.1351(2)	1.3117(5)	2.29(5)
N	1.0077(4)	0.3800(3)	0.1168(6)	3.40(7)
C(1)	1.3634(3)	−0.0531(3)	1.1149(6)	1.80(6)
C(2)	1.3345(3)	0.0560(3)	0.9077(6)	1.60(6)
C(3)	1.4713(3)	0.1032(3)	0.8085(6)	1.72(6)
C(4)	0.8761(5)	0.4578(3)	0.1292(7)	3.23(9)
C(5)	0.8711(5)	0.5781(4)	0.0125(8)	3.69(9)
C(6)	0.7368(6)	0.4092(5)	0.269(1)	4.7(1)
(b) β-{[Cu(CA)(H$_2$O)$_2$](dmpyz)}$_n$ (**1b**)				
Cu	1.0000	0.0000	1.0000	1.54(1)
Cl	1.6050(1)	0.23127(9)	0.6021(2)	2.21(2)
O(1)	0.7555(3)	−0.0857(2)	1.2261(4)	1.92(5)
O(2)	0.8422(3)	0.1022(2)	0.87784)	1.69(5)
O(3)	1.1454(4)	0.1607(3)	1.2841(5)	2.28(6)
N	0.9437(4)	−0.3927(3)	1.5824(6)	2.21(7)
C(1)	0.6807(4)	0.0586(3)	0.9288(6)	1.43(6)
C(2)	0.6295(4)	−0.0523(3)	1.1237(6)	1.45(7)
C(3)	0.5500(4)	0.1065(3)	0.8226(6)	1.44(7)
C(4)	0.8691(5)	−0.4741(4)	1.3476(7)	2.05(8)
C(5)	1.0729(5)	−0.4201(4)	1.7310(7)	2.12(8)
C(6)	0.7192(7)	−0.4490(6)	1.1800(10)	3.9(1)
(c) {[Cu(CA)(H$_2$O)$_2$](phz)}$_n$ (**2**)				
Cu	1.0000	0.0000	0.0000	1.58(1)
Cl	0.58633(1)	−0.19319(7)	0.4226(2)	2.37(2)
O(1)	0.7504(3)	0.0851(2)	−0.1823(4)	2.22(5)
O(2)	0.8282(2)	−0.0786(2)	0.1682(4)	2.04(5)
O(3)	1.0063(3)	0.1246(2)	0.3162(5)	2.20(6)
N	1.0048(3)	0.3758(2)	0.4049(5)	2.27(6)
C(1)	0.6298(4)	0.0483(3)	−0.1043(6)	1.62(6)
C(2)	0.6719(4)	−0.0485(3)	0.0981(6)	1.61(6)
C(3)	0.5413(4)	−0.0882(3)	0.1906(6)	1.73(7)
C(4)	0.7126(5)	0.4035(3)	0.8913(8)	2.90(8)
C(5)	0.8063(4)	0.3544(3)	0.6971(8)	2.71(8)
C(6)	0.9059(4)	0.4263(3)	0.5895(7)	2.20(7)
C(7)	1.0985(4)	0.4474(3)	0.3148(7)	2.16(7)
C(8)	1.2014(4)	0.3990(3)	0.1130(7)	2.61(8)
C(9)	1.2918(4)	0.4718(3)	0.0139(8)	2.80(8)
(d) {[Cu(CA)(H$_2$O)](ohphz)}$_n$ (**7**)				
Cu(1)	0.0000	0.3986(2)	0.2500	2.37(7)
Cl(1)	0.5000	0.4270(3)	0.4296(2)	3.2(1)
O(1)	0.0000	0.246(1)	0.2500	3.6(4)
O(2)	0.1896(8)	0.4148(5)	0.3237(4)	2.5(2)
N(1)	0.322(2)	0.1561(9)	0.2500	2.6(3)
C(1)	0.5000	0.421(1)	0.3332(9)	2.3(4)
C(2)	0.342(1)	0.4178(7)	0.2941(5)	1.7(2)
C(4)	0.409(1)	0.1551(7)	0.1833(6)	2.4(3)
C(5)	0.309(1)	0.1525(8)	0.1089(6)	3.5(3)
C(6)a	0.421(3)	0.165(2)	0.037(1)	2.5(5)
C(7)a	0.412(3)	0.111(2)	0.044(1)	3.3(5)

[a] Disordered carbon atoms with site occupancies of 50%. $B_{eq} = 8/3\pi^2(U_{11}(aa^*)^2 + U_{22}(bb^*)^2 + U_{33}(cc^*)^2 + 2U_{12}aa^*bb^*(\cos\gamma) + 2U_{13}aa^*cc^*(\cos\beta) + 2U_{23}bb^*cc^*(\cos\alpha))$.

dmpyz molecule is not directly coordinated to the copper atom but the two nitrogen atoms are linked to the nearest-neighbor coordinated waters by hydrogen bonding (N···O = 2.740(3) Å).

The crystal packing structure consists of stacking columns of dmpyz molecules and straight $[Cu(CA)(H_2O)_2]_k$ chains, which run along the *c*- and *a*-axes, respectively. This column and chain are vertical to each other (Figure 1c). On the other hand, $\{[M(CA)_2(H_2O)_3]\cdot H_2O\}_n$ (M = Ca^{2+}, Sr^{2+}), $\{[M(Br_2DHBQ)_2(H_2O)_3]\cdot H_2O\}_n$ (M = Ca^{2+}, Sr^{2+}, Br_2DHBQ = 3,6-dibromo-2,4-dihydroxyquinone), and $[Ca(Et_2DHBQ)_2(H_2O)_3]_n$ consist of corrugated chains,[26,29] and zigzag chains have been found in $\{[Y_2(CA)_3(H_2O)_6]\cdot 6.6H_2O\}_n$[25] and $\{Na_2[M(H_2\text{-}DHBQ)_3]\cdot(H_2O)_{24}\}_n$ (M = Mn^{2+}, Cd^{2+}),[27] where H_2-$DHBQ^{2-}$ dianions link these chains to afford large cavities available for building

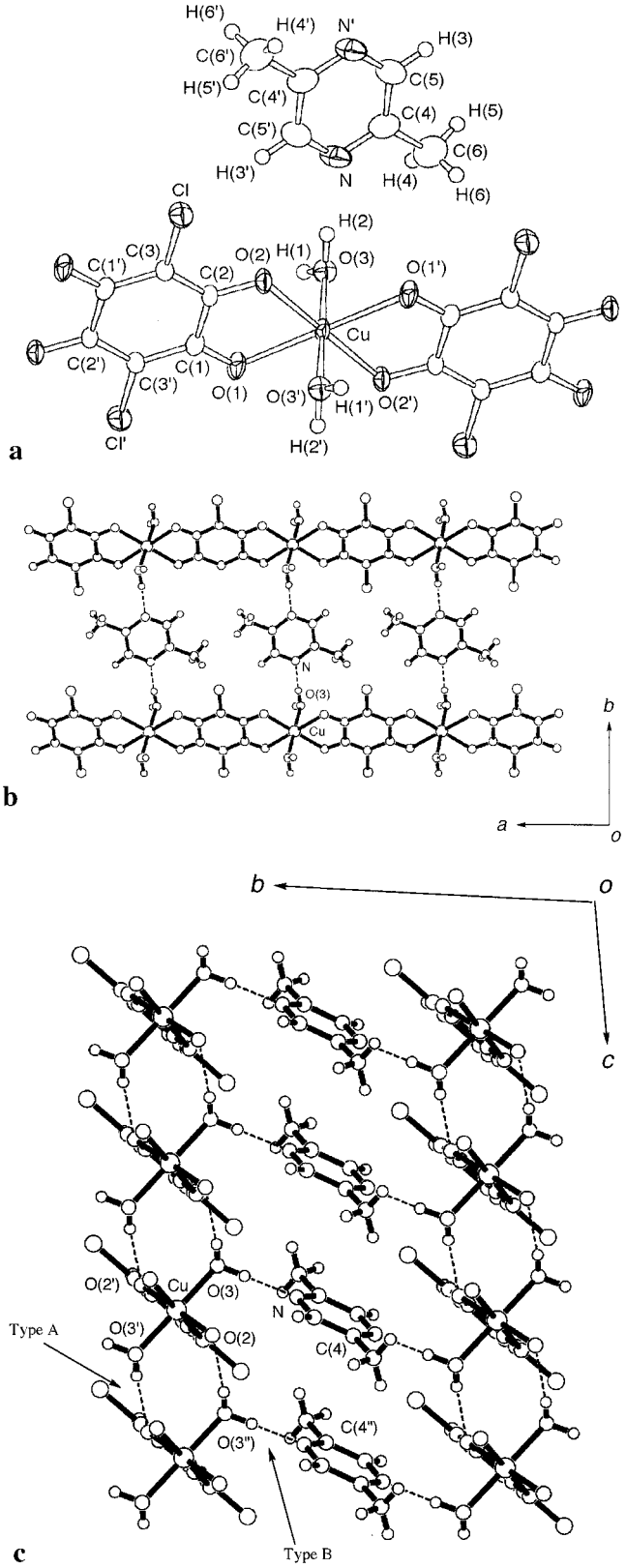

Figure 1. (a) ORTEP drawing of a monomer unit of compound **1a** with labeling scheme and thermal ellipsoids at the 50% probability level for Cu, Cl, O, N, and C atoms. Spheres of the hydrogen atoms have been arbitrarily reduced. The atoms having dashed number are related by a center of inversion at the copper atom or a midpoint of the pyrazine molecule. (b and c) Projection of **1a** along the *c* axis (b) and *a* axis (c). The broken lines denote the sites of hydrogen bonding between the molecules.

Table 3. Selected Bond Distances (Å) and Angles (deg)

(a) α-{[Cu(CA)(H_2O)$_2$](dmpyz)}$_n$ (**1a**)

Distances

Cu−O(1)	2.225(2)	O(2)−C(2)	1.270(3)	C(1)−C(3′)	1.414(3)
Cu−O(2)	2.057(2)	N−C(4)	1.333(4)	C(2)−C(3)	1.377(3)
Cu−O(3)	1.959(2)	N−C(5′)	1.333(4)	C(4)−C(5)	1.386(4)
Cl−C(3)	1.738(3)	C(1)−C(2)	1.534(4)	C(4)−C(6)	1.507(5)
O(1)−C(1)	1.245(3)				

Angles

O(1)−Cu−O(2)	77.04(7)	O(1)−C(1)−C(3′)	123.7(3)	Cl−C(3)−C(2)	119.0(2)
O(1)−Cu−O(3)	93.88(8)	C(2)−C(1)−C(3′)	118.7(2)	C(1′)−C(3)−C(2)	122.6(2)
O(2)−Cu−O(3)	91.05(8)	O(2)−C(2)−C(1)	116.2(2)	N−C(4)−C(5)	119.5(3)
Cu−O(1)−C(1)	111.6(2)	O(2)−C(2)−C(3)	125.2(3)	N−C(4)−C(6)	117.7(3)
Cu−O(2)−C(2)	117.1(2)	C(1)−C(2)−C(3)	118.7(2)	C(5)−C(4)−C(6)	122.7(4)
O(1)−C(1)−C(2)	117.6(2)	Cl−C(3)−C(1′)	118.4(2)	N′−C(5)−C(4)	122.9(3)

Hydrogen Bond Distances and Angles

O(2)-O(3′)	2.724(3)	O(2)-H(1′)-O(3′)	168(3)	O(3)-H(2)-N	177(3)
O(3)-N	2.740(3)				

(b) β-{[Cu(CA)(H_2O)$_2$](dmpyz)}$_n$ (**1b**)

Distances

Cu−O(1)	2.323(2)	O(2)−C(1)	1.267(4)	C(1)−C(3)	1.383(4)
Cu−O(2)	1.982(2)	N−C(4)	1.337(4)	C(2)−C(3′)	1.401(4)
Cu−O(3)	1.970(2)	N−C(5)	1.334(4)	C(4)−C(5′)	1.376(5)
Cl−C(3)	1.734(3)	C(1)−C(2)	1.539(4)	C(4)−C(6)	1.500(5)
O(1)−C(2)	1.250(3)				

Angles

O(1)−Cu−O(2)	76.16(8)	O(2)−C(1)−C(3)	124.3(3)	Cl−C(3)−C(2′)	118.3(2)
O(1)−Cu−O(3)	92.69(10)	C(2)−C(1)−C(3)	118.6(3)	C(1)−C(3)−C(2′)	122.4(3)
O(2)−Cu−O(3)	91.50(10)	O(1)−C(2)−C(1)	116.1(3)	N−C(4)−C(5′)	119.8(3)
Cu−O(1)−C(2)	108.9(2)	O(1)−C(2)−C(3′)	124.9(3)	N−C(4)−C(6)	118.2(3)
Cu−O(2)−C(1)	119.2(2)	C(1)−C(2)−C(3′)	119.0(3)	C(5′)−C(4)−C(6)	122.0(4)
C(4)−N−C(5)	117.0(3)	Cl−C(3)−C(1)	119.3(2)	N−C(5)−C(4′)	123.2(3)
O(2)−C(1)−C(2)	117.2(3)				

Hydrogen Bond Distances and Angles

O(1)−O(3′)	2.799(3)	O(1)−H(1′)−O(3′)	171(4)	O(3)−H(2)−N	174(4)
O(3)−N	2.769(3)				

(c){[Cu(CA)(H_2O)$_2$](phz)}$_n$ (**2**)

Distances

Cu−O(1)	2.228(2)	C(2)−C(3)	1.377(4)	N−C(7)	1.336(4)
Cu−O(2)	2.073(2)	C(3)−C(1′)	1.414(4)	C(7)−C(8)	1.421(4)
Cu−O(3)	1.963(2)	C(3)−Cl	1.732(3)	C(8)−C(9)	1.351(5)
O(1)−C(1)	1.241(3)	C(4)−C(5)	1.347(5)	C(4)−C(9′)	1.418(5)
O(2)−C(2)	1.275(3)	C(5)−C(6)	1.419(4)	C(6)−C(7′)	1.436(4)
C(1)−C(2)	1.533(4)	C(6)−N	1.342(4)		

Angles

O(1)−Cu−O(2)	76.38(7)	C(1)−C(2)−C(3)	118.7(3)	C(7′)−C(6)−N	121.0(3)
O(2)−Cu−O(3)	87.80(9)	C(2)−C(3)−C(1′)	122.3(3)	C(6)−N−C(7)	117.4(3)
O(3)−Cu−O(1)	90.32(10)	C(2)−C(3)−Cl	119.4(2)	N−C(7)−C(6′)	121.6(3)
Cu−O(1)−C(1)	113.0(2)	C(9′)−C(4)−C(5)	120.7(3)	C(6′)−C(7)−C(8)	118.8(3)
Cu−O(2)−C(2)	117.4(2)	C(4)−C(5)−C(6)	120.3(3)	C(7)−C(8)−C(9)	119.9(3)
C(3′)−C(1)−C(2)	119.0(3)	C(5)−C(6)−C(7′)	119.0(3)	C(8)−C(9)−C(4′)	121.3(3)

Hydrogen Bond Distances and Angles

O(2)−O(3′)	2.779(3)	O(2)−H(1′)−O(3′)	169(3)	O(3)−H(2)−N	158(3)
O(3)−N	2.803(3)				

(d){[Cu(CA)(H_2O)](ohphz)}$_n$ (**7**)

Distances

Cu(1)−O(1)	2.12(2)	C(1)−C(2)	1.39(1)	C(5)−C(6)	1.53(2)
Cu(1)−O(2)	1.955(6)	C(2)−C(2C)	1.56(2)	C(6)−C(6B)	1.21(4)
Cl(1)−C(1)	1.71(2)	C(4)−C(4B)	1.38(2)	C(5)−C(7)	1.50(2)
O(2)−C(2)	1.27(1)	C(4)−C(5)	1.52(1)	C(7)−C(7B)	1.34(4)
N(1)−C(4)	1.35(1)				

Angles

O(1)−Cu(1)−O(2)	96.6(2)	C(2)−C(1)−C(2B)	120(1)		
O(2)−Cu(1)−O(2A)	83.5(4)	O(2)−C(2)−C(1)	125.9(9)	C(4)−C(5)−C(6)	116(1)
O(2)−Cu(1)−O(2C)	95.0(4)	O(2)−C(2)−C(2C)	114.3(5)	C(5)−C(6)−C(6)	123.7(9)
Cu(1)−O(2)−C(2)	113.7(6)	C(1)−C(2)−C(2C)	119.8(7)	C(4)−C(5)−C(7)	114(1)
C(4)−C(4B)−C(5)	120.1(6)				
C(4)−N(1)−C(4C)	121(1)	N(1)−C(4)−C(4B)	119.3(6)	C(5)−C(7)−C(7)	121.4(9)
Cl(1)−C(1)−C(2)	119.9(7)	N(1)−C(4)−C(5)	120.6(9)		

Hydrogen Bond Distances and Angles

O(1)−N(1)	2.75(1)	O(1)−H(3)−N(1)	169.4

zeolite- or clathrate-like structures.[66] The difference in the chain structure between **1a** and those compounds is due not only to the coordination number of the metal atom but also to the Jahn−Teller distortion around the metal characteristic of copper.

Interestingly, the chains, $\{[Cu(CA)(H_2O)_2]_k\}_l$, in **1a** are linked by two types of hydrogen bonds; the type A is for forming a sheet and type B is for connecting sheets, as is shown in Figure 1c. The type A hydrogen bond (O(2)−O(3″) = 2.724(3) Å) occurs between the coordinated water and the oxygen atom of the CA^{2-} anion on the adjacent chain, and links the chains to form a sheet spreading out along the *ac*-plane. A similar connectivity has been found in $\{[Ca(Et_2DHBQ)_2]\cdot 3H_2O\}_n$,[29] where the hydrogen bonding distance (3.094(7) Å) is longer than that of **1a**. The crystal structure of $\{[Ca(Et_2DHBQ)_2]\cdot 3H_2O\}_n$ is, however, different from that of **1a** because of the large coordination number of the Ca(II) ion. The sheet structure of **1a** is similar to that of **4**,[41] whose hydrogen bond (O--O distance: 2.845(3) Å) occurs between the apically coordinated CH_3OH and the oxygen atom of CA^{2-} in the nearest-neighbor chain. The compound **4** contains the only type A hydrogen bonding because methanol is a monohydric alcohol while in **1a** the remaining H atom of H_2O can be utilized to connect sheets. Compound **6** is a typical example of this role of H_2O.[43,44] The sheet structure in **1a** differs from the notched sheet structure of **6**. This is due to the variety of the hydrogen bonding capability of the interstitial water molecule, which has two H-donor and two H-acceptor sites. The intercalated guest molecules also affect the sheet structure of $\{[Cu(CA)(H_2O)_2]_k\}_l$.

The type B hydrogen bonding occurs between the uncoordinated dmpyz and the coordinated water (N−O(3) = 2.740(3) Å). Interestingly, $\{[Cu(CA)(H_2O)_2]_k\}_l$ sheets sandwich dmpyz molecules, which serve not as a linking ligand but as a proton acceptor. This hydrogen bond interlinks the nearest-neighbor sheets to afford a three-dimensional structure and, in other words, provides a novel stoichiometric intercalation compound. These dmpyz molecules are stacked with the interplanar distance of 3.67 Å and the nearest neighbor C(4)−C(4″) distance of 3.763(7) Å along *c*-axis, perpendicular to the $[Cu(CA)(H_2O)_2]_n$ chains and the plane of a dmpyz molecule tilts to the stacking direction by 39.8°. Subsequent stacks are related by translations. The geometry of the dmpyz molecule is similar to that of coordinated dmpyz molecules.[10,50,67−70]

Crystal Structure of 1b. An ORTEP drawing of the structure around the copper in **1b** with the atom numbering scheme is shown in Figure 2a, where the copper atom sits on the crystallographic inversion center. The selected bond distances and angles with their estimated standard deviations are listed in Table 3. A layered structure having two types of hydrogen bonding as well as **1a** is shown in parts b and c of Figure 2. The straight chains of $\{[Cu(CA)(H_2O)_2]_k\}_l$ are interlinked by hydrogen bonds between the coordinated water and the oxygen atoms of CA^{2-} on the adjacent chain, forming a two-dimensional sheet, which spread out along the *ac*-plane. **1b** shows a hydrogen bonding distance (O(1)--O(3″) = 2.799(3) Å) longer than that of **1a** (2.724(3) Å), reflecting the longer length of the *c*-axis. The geometry around the copper atom is an elongated octahedron (4 + 2 type) with four short distances

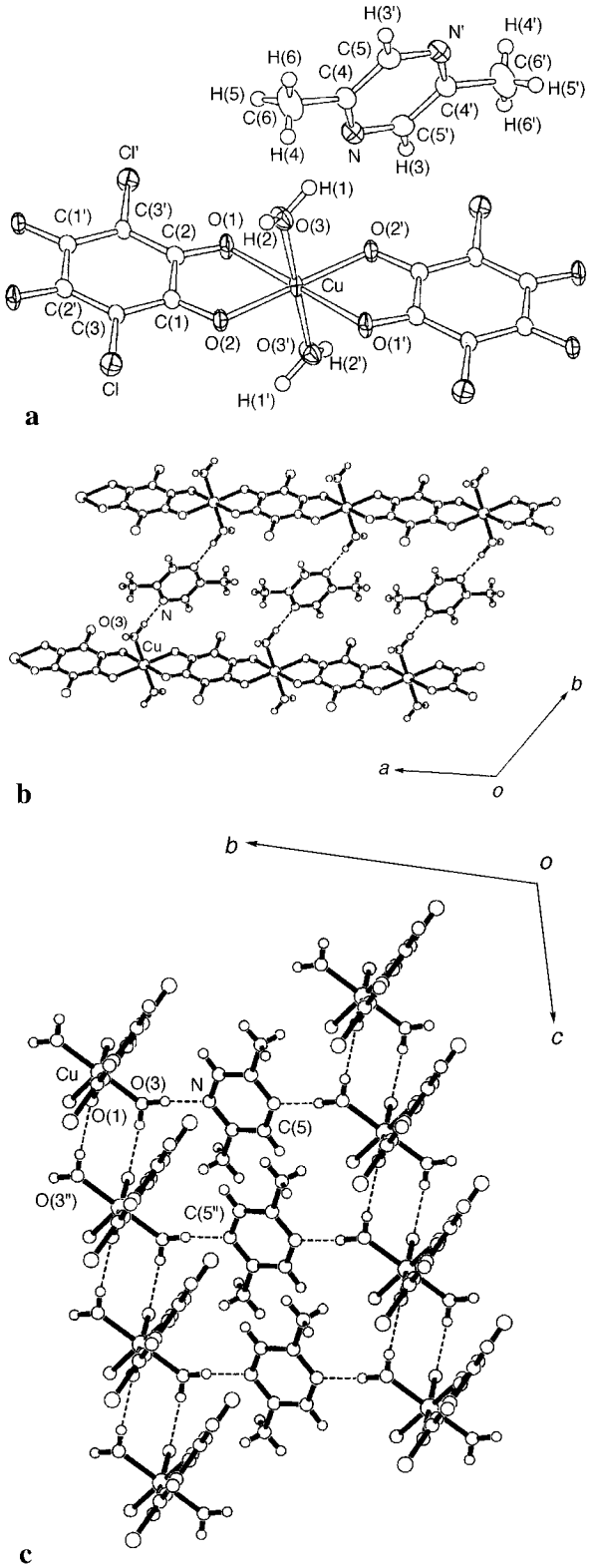

Figure 2. (a) ORTEP drawing of a monomer unit of compound **1a** with labeling scheme and thermal ellipsoids at the 50% probability level for Cu, Cl, O, N, and C atoms. Spheres of the hydrogen atoms have been arbitrarily reduced. The atoms having dashed number are related by a center of inversion at the copper atom or a midpoint of the 2,5-dimethylpyrazine molecule. (b and c) Projection of **1b** along the *c* axis (b) and *a* axis (c). The broken lines denote the sites of hydrogen bonding between the molecules.

(Cu−O(2), Cu−O(2′) = 1.982(2) Å, and Cu−O(3), Cu−O(3′) = 1.970 Å) and two long distances (Cu−O(1) and Cu−O(1′) = 2.323(2) Å). The atoms of Cu, O(2), O(2′), O(3), and O(3′) form a basal plane, perpendicular to the direction of the Cu−

(66) Meier, W. M.; Olson, D. H. *Atlas of Zeolite Structure Types*; Butterworth-Heinemann: London, 1992.
(67) Otieno, T.; Retting, S. J.; Thompson, R. C.; Trotter, J. *Inorg. Chem.* **1993**, *32*, 1607.
(68) Maveric, A. W.; Ivie, M. L.; Waggenspak, J. H.; Fronczek, F. R. *Inorg. Chem.* **1990**, *29*, 2403.
(69) Otieno, T.; Rettig, S. J.; Thompson, R. C.; Trotter, J. *Can. J. Chem.* **1990**, *68*, 1901.
(70) Ayres, F. D.; Pauling, P.; Robertson, G. B. *Inorg. Chem.* **1964**, *3*, 1303.

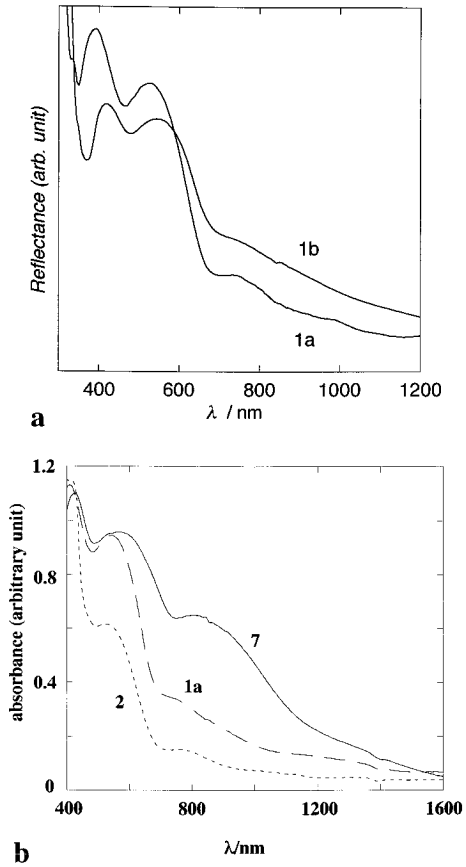

Figure 3. Polycrystalline powder diffuse reflectance spectra of (a) **1a** and **1b** and (b) **1a**, **2**, and **7**.

CA chain. The distortion, (d(Cu−O(2)) − d(Cu−O(3)) = 0.01 Å), from a tetragonal configuration is much smaller than that from the rhombic copper environment of **1a** (0.1 Å). These structural isomers are in good contrast to each other. It is worth noting that the type A hydrogen bonding between chains of **1b** occurs in the apical oxygen atom O(1), resulting in the elongation of the Cu−O(1) distance whereas the hydrogen bonding in **1a** is noticed in the basal oxygen atom, O(2). This

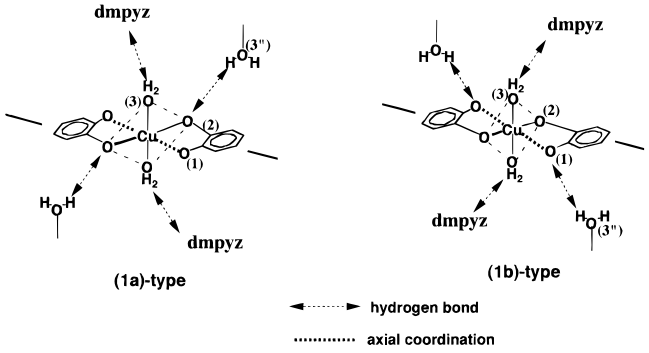

site difference in the chain linkage influences not only the Cu−O(CA) distances but also the chain zigzag mode; the Cu−O(1)−O(2) moiety is folded at a O(1)−O(2) hinge and the dihedral angles (γ) between the least-squares planes of Cu−O(1)−O(2) and O(1)−O(2)−C(1)−C(2) are 173.7 (**1a**), 166.6 (**1b**), and 179.9° (**2**) (*vide infra*), respectively.

The dmpyz molecules are also intercalated between the sheets but the mode is dissimilar to that of **1a**. The differences between **1a** and **1b** are recognized in a stack of dmpyz molecules together with the hydrogen bond distance (N---O(3) = 2.769(4) Å) being slightly longer than that of **1a** (2.740(3) Å). The dmpyz molecule is canted to the stacking direction by 54.7° (Figure

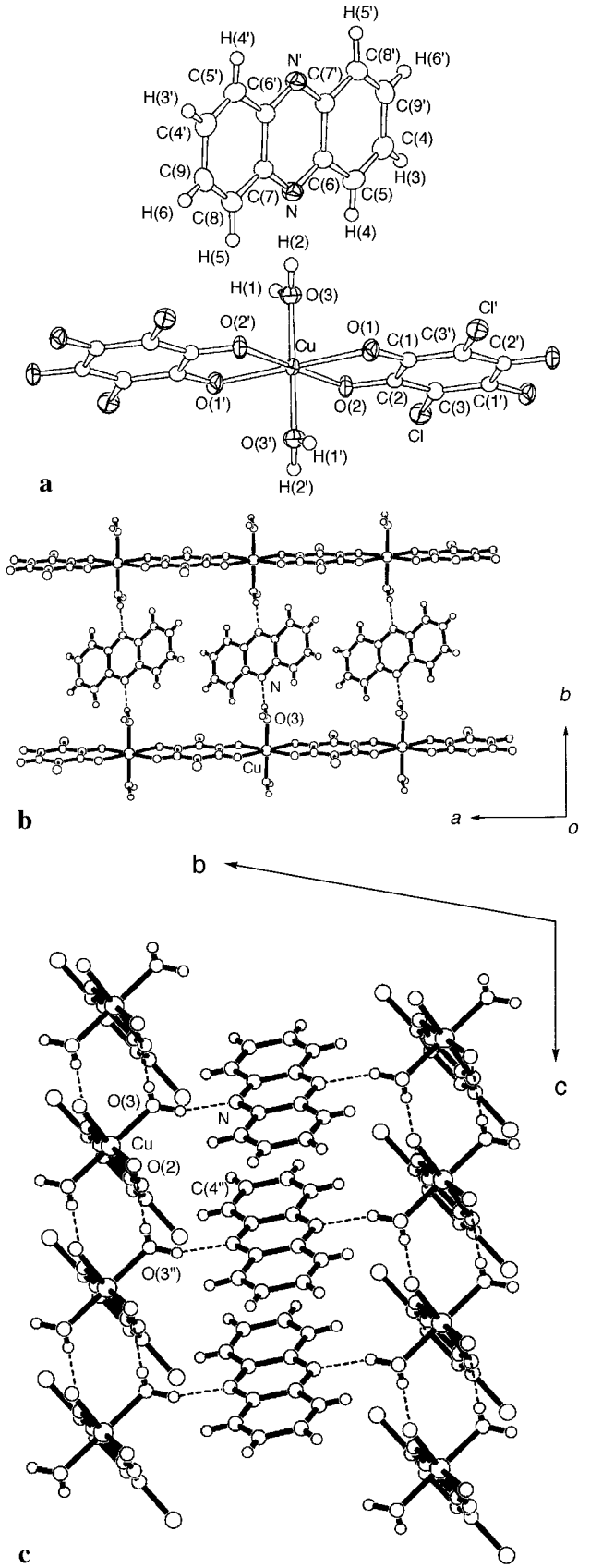

Figure 4. (a) ORTEP drawing of a monomer unit of compound **2** with labeling scheme and thermal ellipsoids at the 50% probability level for Cu, Cl, O, N, and C atoms. Spheres of the hydrogen atoms have been arbitrarily reduced. The atoms having dashed number are related by a center of inversion at the copper atom or a midpoint of the phenazine molecule. (b and c) Projection of **2** along the *c* axis (b) and *a* axis (c). The broken lines denote the sites of hydrogen bonding between the molecules.

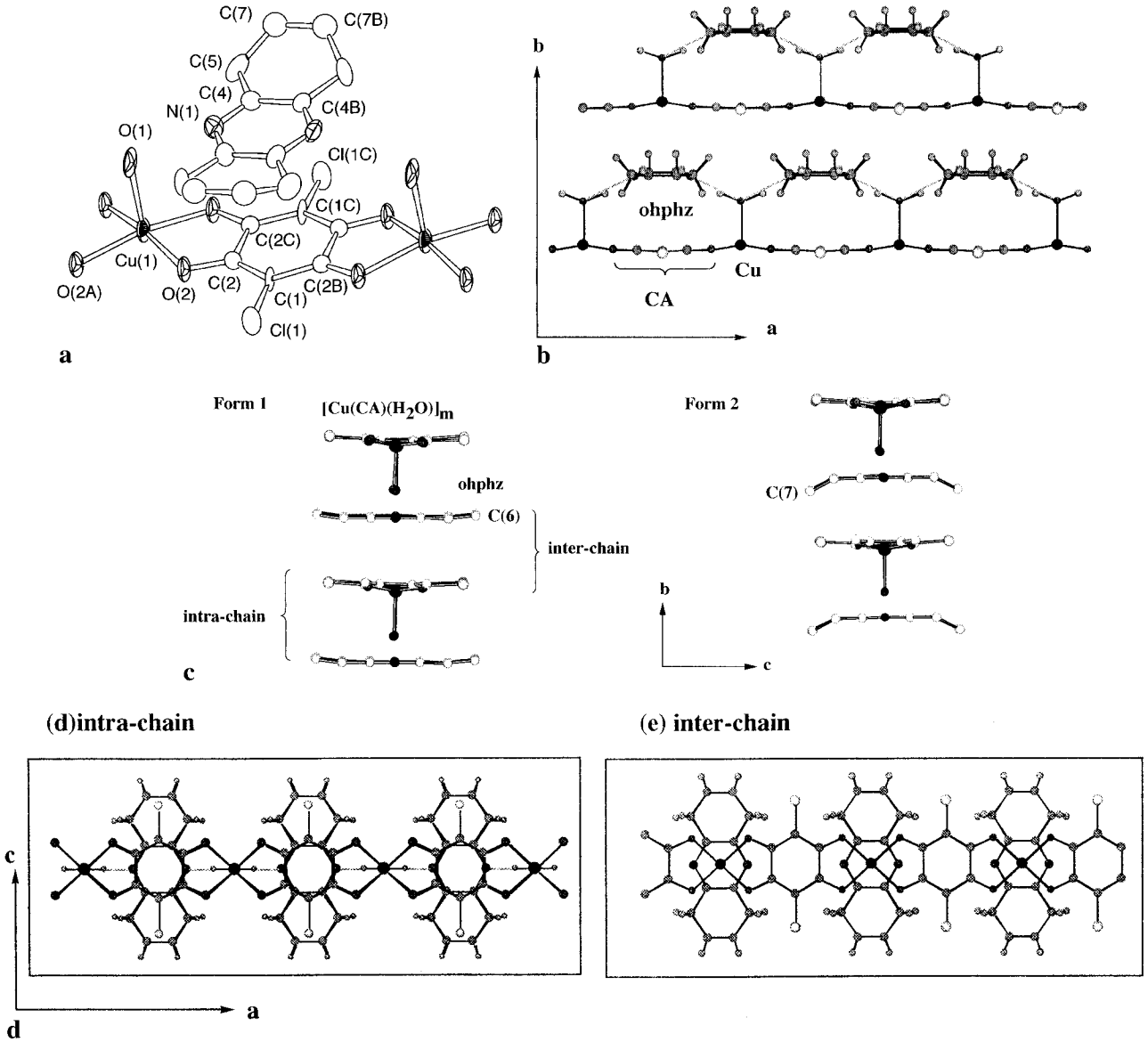

Figure 5. ORTEP drawing of a monomer unit (a) of compound **7** with labeling scheme and thermal ellipsoids at the 50% probability level for Cu, Cl, O, N, and C atoms. One of the two disordered form for the ohphz molecule is drawn. The hydrogen atoms are omitted. The atoms having dashed number are related by a mirror plane. The relationship between the chains and ohphz molecules are shown by the figures projected down the *c* (b), *a* (c), and *b* (d) axis. Part c exhibits the two disordered forms. The intra- and interchain relationships of the ohphz with the attached chain or the neighboring chain are shown in part d.

2b,c). The nearest carbon−carbon distance (C(5)−C(5″) = 3.430(7) Å) is shorter than that of **1a**; however the overlapping area of dmpyz in **1b** is much smaller than that of **1a**. This kind of polymorphism is also seen in organic molecular crystals such as a 4,4′-bipyridinium salt of squaric acid, and the two phases are connected by proton transfer which influences the electron donor−acceptor properties of the participating ions.[57] In compounds **1a** and **1b**, although the phenomenon is not directed to proton transfer, the coordination geometry around the copper strongly correlates to the hydrogen bonding interaction, which is reflected by the appreciable difference in color between red purple (**1a**) and brown (**1b**) (Figure 3).

Crystal Structure of 2. An ORTEP drawing of the structure around the copper in **2** with the atom numbering scheme is shown in Figure 4a, and selected bond distances and angles with their estimated standard deviations are listed in Table 3. The geometry around the copper atom is a distorted elongated octahedron (2 + 2 + 2) type with three pairs of different Cu−O distances: 2.228(2) Å (Cu−O(1) and Cu−O(1′)), 2.073(2) Å (Cu−O(2), Cu−O(2′)), and 1.963(2) Å (Cu−O(3), Cu−O(3′)). The rhombic distortion around the copper is recognized on the basis of the difference in the bond distance (d(Cu−O(2)) − d(Cu−O(3) = 0.1 Å), indicating that geometric and electronic structure of **2** is close to that of **1a**.

A layered structure which is supported by hydrogen bonding interaction is also shown in **2** (Figure 4c). The straight chains of $[Cu(CA)(H_2O)_2]_n$ are interlinked between the coordinated water and the oxygen atoms of CA^{2-} on the adjacent chain, forming a two dimensional sheet, which spread out along the *ac*-plane. The water oxygen atom (O(3)) in **2** is hydrogen bonded to the basal CA oxygen atom in the adjacent chain with a distance, O(2)--O(3″), of 2.779(3) Å, longer than that of **1a** but the same order of magnitude as that in **1b**. This hydrogen bonding is classified as a **1a** type linkage. Coplanarity of the Cu-CA chain in **2** (γ = 179.9°) is found in a much higher degree than that of the other polymers.

The intercalated mode of phz molecules, which is stabilized by N−O(3) hydrogen bonding, is similar to that of **1a**. They are stacked along the *c*-axis perpendicular to the [Cu(CA)-$(H_2O)_2$] chain (the interplanar distance of 3.18 Å and nearest neighbor N−C(4″) distance of 3.203(5) Å) and the plane of the phz molecule is tilted to the stacking direction by 48.8°,

forming a column structure in between the $\{[Cu(CA)(H_2O)_2]_k\}_l$ layers (Figure 4c). Subsequent stacks are related by translations. Each phz molecule has an ordinary geometry as does the free molecule. The stacking distance is shorter than the distance in the graphite, indicating that there is expected to be a large $\pi-\pi$ interaction between each phz molecule.

Crystal Structure of 7. An ORTEP drawing of the structure around the copper in **7** with the atom numbering scheme is shown in Figure 5a, and selected bond distances and angles with their estimated standard deviations are listed in Table 3. The copper atom displays a five-coordinate square-pyramidal configuration with four equatorial oxygen atoms of the two CA molecules and one apical oxygen atom of the water molecule, the distances Cu−O(2) and Cu−O(1) being 1.955(6) and 2.12-(2) Å, respectively. The copper atom deviates by 0.23 Å from the center of the basal plane of the four oxygen atoms. The chain of $[Cu(CA)(H_2O)_2]_n$ shows a slight zigzag mode, tilting by 7° at the hinge formed by O(2) and O(2′) as is shown in Figure 5b. It is to be noted from Figure 5b,c that there are no hydrogen-bonding links between chains, dissimilar to **1a**−**6**.

The ohphz molecules are intercalated in between chains. Each ohphz is anchored by the N(1)−O(1) and N(1′)−O(1′) hydrogen bonding in a manner parallel to the chain direction. Certain attractive interactions between ohphz and CA molecules in a chain are hinted at due to the short interplanar distance (e.g. N---C(1) distance of 3.7 Å), whereas there is no chain−chain interaction through ohphz molecules according to the overlapping mode (Figure 5d). Therefore, ohphz molecules play no role in interlinking chains, leading to the thermal instability of the crystals. Each ohphz molecule has the bond distances and angles similar to those of a free molecule as is found in the corresponding 1,9-dichloro-1,2,3,4,6,7,8,9-octahydrophenazine 5-oxide.[71]

Intercalation Modes of the Guest Molecules. We have found the two types of intercalation modes of guest molecules: (1) chains-linking type in **1a**, **1b**, and **2** and (2) chain-sticking type in **7**. For type 1 the guest molecules, dmpyz and phz, which have a planar and π-conjugated structure, are stacked along *c*-axis perpendicular to the $[Cu(CA)(H_2O)_2]_n$ chain, forming a slipped stack column in between the layers of $\{[Cu(CA)(H_2O)_2]_k\}_l$. The layer structure, which is built by the hydrogen bonding between the coordinated waters and chloranilates, influences the column structure, in particular the repetition distance and the degree in the slipped stack form, the latter characterized by a tilt angle, α, regarding the molecular plane to the stacking direction. The α values are 39.8° (**1a**), 54.7° (**1b**), and 48.8° (**2**). The stacking distance of phz in **2** is shorter than that of carbon layers in graphite and that of free phenazine.[72−76] The neighboring phz molecules in a stack of **2** have a bond-over-ring arrangement, characteristic of favorable interaction, which is also found in superconducting κ-phase BEDT-TTF salts.[57] In the case of dmpyz the stack arrangement is less effective than that in phz case, but the $\pi-\pi$ interaction is still expected.

Let us now return to type 2 in **7**. By the anchor effect of the hydrogen bonding, the ohphz molecules cling to a $[Cu(CA)(H_2O)]_k$ chain in a parallel fashion instead of a stack column, and therefore the ohphz molecules play no role in interlinking chains. A pyrazine moiety of each ohphz sits over a CA with the distance of 3.7 Å in a chain (Figure 5b), to which it clings; an additional $\pi-\pi$ interaction between ohphz and CA molecule in a chain would be expected, whereas regarding a pyrazine−chloranilate ring overlap this moiety is at out-of-phase position to the neighboring chain, indicative of no interchain stacking interaction. Ohphz is a derivative of pyrazine with two bulky cyclohexane substituents on the both sides, which appears to be unfavorable for forming a stack in crystal.

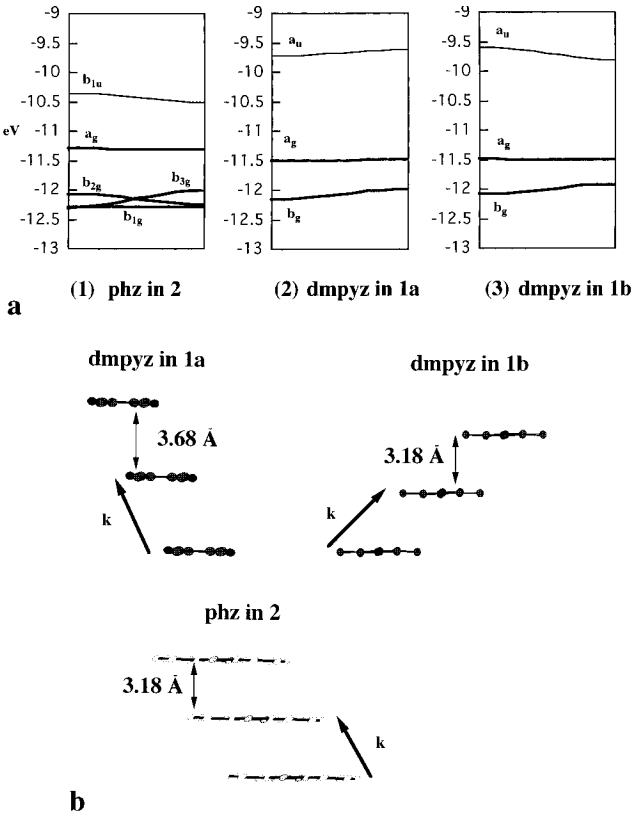

Figure 6. (a) Band structures of the stacked molecules in **2** (phz), **1a** (dmpyz), and **1b** (dmpyz), respectively. (b) The mode of stack projected down the axis perpendicular to the molecular planes. The distances denote that of the translational vector and that of the two molecular planes.

The crystallographic structures imply that in addition to having a hydrogen-bonding support the stack-capability of an intercalated guest molecule is important for a column structure. It is worthwhile to examine the electronic effect of column structure by the band calculations of the slipped stacks of dmpyz and phz extracted from the structures of **1a**, **1b**, and **2**. The band structures are shown in Figure 6, together with the stacking mode and the translational vectors. The molecules dmpyz and phz have C_{2h} and D_{2h} symmetry, respectively. All the bands assigned to a_g, located at Fermi level, indicate no dispersion. This is because these bands are mainly composed of a lone-pair orbital of the N atom oriented to the hydrogen atom of the coordinated water molecule. Bands between −11.5 and −12.5 eV are mainly composed of pπ orbitals with symmetry of b_g for dmpyz and b_{2g}, b_{3g} for phz**.** The bands with a_u and b_{1u} symmetry are ascribed to π^* type orbitals for dmpyz and phz, respectively. The π bands of the phz column exhibits a dispersion (width of 0.3 eV) larger than those (0.17 and 0.16 eV) for dmpyz columns in **1a** and **1b**, respectively. This is accounted for by a short stack distance and a large size of π structure to gain an effective overlapping. The π band profiles for dmpyz in **1a** and **1b** are very close to each other although the stack mode of dmpyz in **1a** and **1b** is different from each other. The stack distance in **1a** is longer than that in **1b** whereas

(71) Galdecki, Z.; Grochulski, P.; Wawrzak, Z. *Acta Crystallogr., Sect. C* **1984**, *C40*, 415.
(72) Herbstein, F. H.; Schmidt, G. M. J. *Acta Crystallogr.* **1955**, *8*, 406.
(73) Herbstein, F. H.; Schmidt, G. M. J. *Acta Crystallogr.* **1955**, *8*, 399.
(74) Hirshfeld, F. L.; Schmidt, G. M. J. *J. Chem. Phys.* **1957**, *26*, 923.
(75) Glazer, A. M. *Philos. Trans. R. Soc. London, Ser. A* **1970**, *266*, 593.
(76) Wozniak, K.; Hariuki, B.; Jones, W. *Acta Crystallogr., Sect. C* **1991**, *47*, 1113.

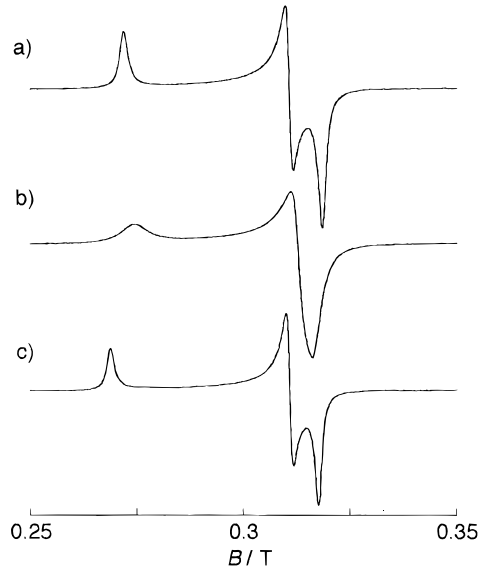

Figure 7. Polycrystalline powder ESR spectra of **1a** (a), **1b** (b), and **2** (c) at 8 K and $\nu = 9.157$ GHz.

the overlapping projection along the axis perpendicular to the molecular plane shows that the mode in **1a** is more effective than that in **1b**.

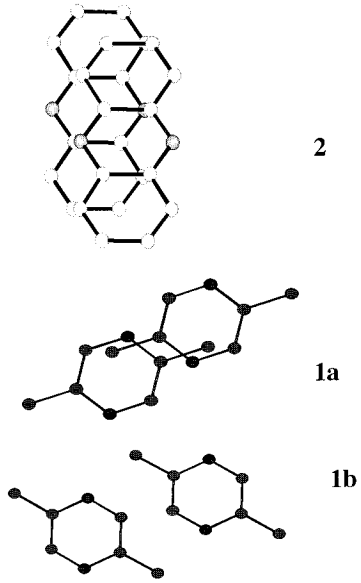

The two spatial parameters of the stacking mode, a distance and an overlap arrangement, for band formation compensate each other so that the intermolecular interaction gives rise to a similar electronic structure of the stack column. There is flexibility of the stacking mode to a certain extent that may optimize the attractive interaction and stabilize the column structure.

Magnetic and Thermal Properties. The compounds **1a**, **1b**, and **2**, were also obtained as polycrystalline phase. The powder diffraction patterns of the compounds are in good agreement with those reproduced by the single-crystal crystallographic data, indicating that each powder sample is essentially the same as the corresponding single-crystal compound.

The ESR spectra in Figure 7 of the polycrystalline samples consist of two or three g values (**1a**, 2.404, 2.104, and 2.053; **1b**, 2.387, 2.071; **2**, 2.434, 2.105, and 2.059), exhibiting no hyperfine structures and sharp line widths, characteristic of the significant exchange narrowing. The degrees of line-narrowing slightly differ in each sample, depending on the exchange

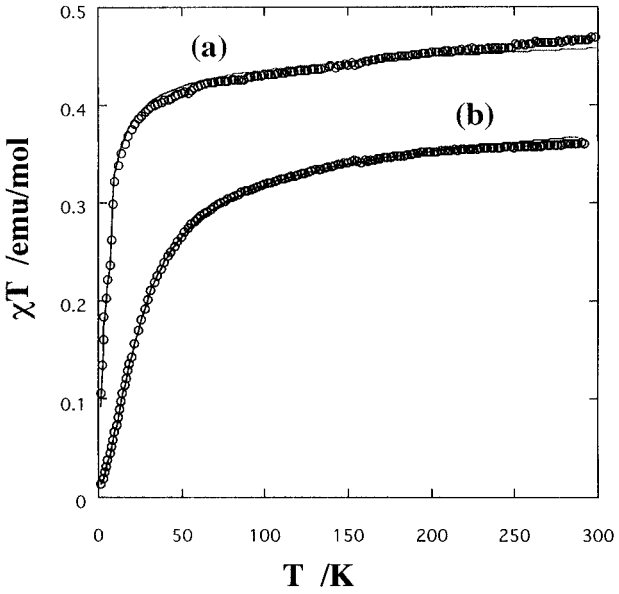

Figure 8. Plots of $\chi_M T$ vs T for **2** (a) and **7** (b). Solid line: theoretical fit of the data with the parameters listed in the text.

interaction. The spectra of **1a** and **2** show a rhombic pattern, which shows the existence of partial mixing of the d_{z^2} orbital into the $d_{x^2-y^2}$ magnetic orbital, while **1b** affords the axial spectrum pattern, indicative of the negligible mixing of d_{z^2} orbital to the magnetic orbital. This ESR aspect is in fairly good agreement with the copper geometries obtained from the crystal structures.

The magnetic susceptibilities (χ) were measured over temperatures of 2−300 K. χT in all cases decreases at lower temperature indicative of antiferromagnetic exchange coupling leading to a singlet ground state. The data were analyzed by using the Heisenberg linear chain theory to give the fitting with $J = -1.83$ cm^{-1}, $g = 2.18$ (**1a**), $J = -0.39$ cm^{-1}, $g = 2.14$ (**1b**), $J = -1.84$ cm^{-1}, $g = 2.18$ (**2**), and $J = -10.93$ cm^{-1}, $g = 2.00$ (**7**). For instance, both the measured and analyzed data of **1b** and **7** are shown in Figure 8. The absolute values of J for **1a**, **1b**, and **2** are smaller than that value for $[Cu(CA)]_n$, which has a planar ribbon structure (−12.3 cm^{-1}),[30] suggesting that the magnetic orbital $d_{x^2-y^2}$ is no longer simply parallel to chloranilate plane but a plane of Cu−O(H_2O) and Cu−O(CA) vectors, which have short bond distances. Thus the coordinated water molecules make the reversal of the magnetic orbital. It is worth noting that the J value of the five-coordinate compound **7** is comparable to that of the $[Cu(CA)]_n$. According to the magnitude of J, **1a** and **2** could be classified in the same group. Owing to the actual site symmetry D_{2h} around the copper atom, the magnetic orbital is composed of an admixture of $d_{x^2-y^2}$ and d_{z^2}, the latter pointing along the O(1)−Cu−O(1′) axis. In the case of **1a** and **2** the mixing of the d_{z^2} orbital is larger than that of **1b** which is also demonstrated by the ESR spectra. Therefore, the spin density on the O(1) and O(1′) oxygen atoms in **1a** and **2** is larger than **1b**; this accounts for the residual coupling for **1a** and **2**. An analogous phenomenon has been observed for $[Cu(CA)L_2]_n$ (L = NH_3, py, etc.).[30] Although these crystal structures are uncertain, two types of magnetic behavior were observed, and thus it is suggested that this result could arise from small differences in the strength of the bases L, which would control the mixing of the magnetic orbital to modify the residual spin densities on the oxygen atoms of CA^{2-} and hence the magnitude of the intrachain coupling. Interestingly, the compounds obtained here undergo a magnetic interaction tuned by hydrogen bonding. Hydrogen bonds are directional and are thus more likely to enforce an orientation of molecules.

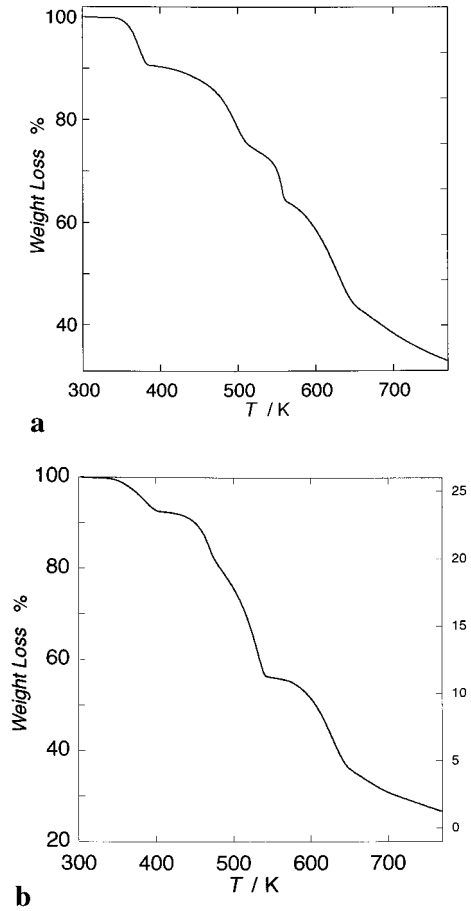

Figure 9. Thermogravimetric analysis data for (a) **1a** and (b) **2**.

Therefore, control of the magnetic interaction is associated with tuning the two-dimensional structure of $\{[Cu(CA)(H_2O)_2]_k\}_l$.

In order to examine the weight loss processes of **1a**, **1b**, and **2**, the thermogravimetric (TG) measurements have been carried out under nitrogen atmosphere. The TG diagram of **1a** is given in Figure 9. Rapid weight loss takes place up to 400 K for all the three compounds. The liberation of two water molecules accounts for this weight loss for **1a** and **1b** (8.7%), and for **2** (7.4%). The obtained species in the intermediate range 400−450 K is thus assigned to $\{[Cu(CA)](X)\}_n$ (X = dmpyz and phz), and the processes of the liberation corresponds to eq 1. The loss of the coordinated water molecules in $[Fe(CA)(H_2O)_2]_n$ has been found near 513 K.[31] In the case of **6** the liberation of both coordinated and interstitial water molecules takes place in the range 400−600 K.[44] Interestingly, the compounds **1a**, **1b**, and **2** release the coordinated water molecules more easily than the intercalated organic molecules, implying the importance of the stacking interaction. The second processes up to 550 K account for 26% (**1a** and **1b**) and 37% (**2**) weight loss and correspond to the liberation of the intercalated molecules (eq 2). The decomposition products of these compounds are

$$\{[Cu(CA)(H_2O)_2](X)\}_n \rightarrow \{[Cu(CA)](X)\}_n + 2H_2O \quad (1)$$

$$\{[Cu(CA)](X)\}_n \rightarrow [Cu(CA)]_n + X \quad (2)$$

assigned to a binary compound, $\{[Cu(CA)]\}_n$, which has been demonstrated by the IR spectrum (ν_{CO} = 1593 cm^{-1}) and XRD. According to the isolation of the 1-D ribbon structure of $\{[Cu(CA)]\}_n$,[30] the framework in these 1-D chains is so stable that no significant destruction of the chain structure occurs upon the release of both coordinated and interstitial water molecules. In the final processes the reactions are thought to be the decomposition of each $[Cu(CA)]_n$.

Control of Crystal Structures. In this study, we have synthesized a series of crystalline copper(II) coordination polymers. They contain two kinds of hydrogen bond type chain-links and a π-type stack column of the guest molecules. All the linkages are well correlated to the formation of the crystal lattice. In order to control the crystal structure, it is instructive to see how these key factors operate in fabrication of crystalline coordination polymers. First, we checked the formation of a hydrogen bond-supported sheet, $\{[Cu(CA)(H_2O)_2]_k\}_l$ (**5**), without any intercalated molecules, which interlink the chains.

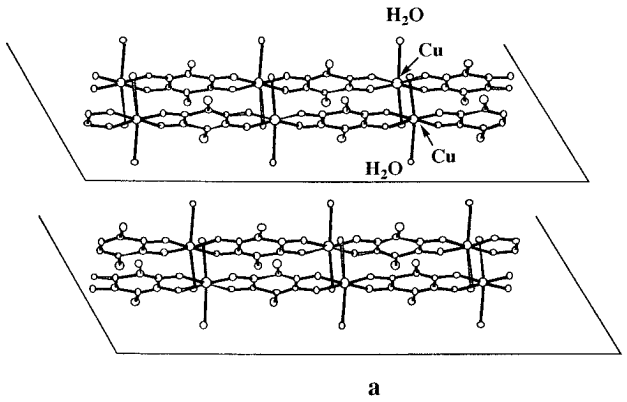

Fortunately, we have succeeded in growing brown crystals of the compound having no guest molecules. The crystal structure indicates a sheet structure as well as **1a**, **1b**, and **2**,[77] consisting of $[Cu(CA)(H_2O)_2]_n$ chains, which are hydrogen-bonded to each other and link the chains to form a flat sheet spreading out along the *ab*-plane. The interlayer distance[78] is about 8.45 Å. The simple layered structure, $\{[Cu(CA)(H_2O)_2]_k\}_l$, thus, can be readily built although the crystal structure is unstable possibly because there are no interchain linkages such as hydrogen bonding. This instability is also found in compound **7**, which has no interchain linkages. All the crystal structures of **1a**, **1b**, **2**, and **6** demonstrate that the 2-D structure of $\{[Cu(CA)(H_2O)_2]_n\}_m$ is a basic framework in the ternary Cu(II)/CA/H_2O system. The interchain distance in the sheet is primarily dependent on the hydrogen bonding, and of course, the geometry around the copper as is found in the polymorphism of **1a** and **1b** and the bonding parameters of the coordinated water molecule are important factors. In practice the hydrogen-bonding distances of O−H---O for **1a**, **1b**, and **2** range from 2.74 to 2.78 Å. In relation to 2-D structures the coordination bond linkage should be mentioned. By using a ternary Cu(II)/CA/pyz system we have also succeeded in the synthesis and the characterizations of a 2-D coordination polymer, $[Cu(CA)(pyz)]_n$ (**3**),[41] in which a coordination bond is utilized to link $[Cu(CA)]_n$ instead of a hydrogen bond via coordinated water.

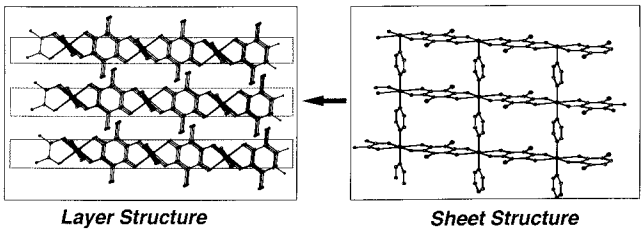

This coordination bond-type polymer is one of good candidates for rational synthesis of 2-D frameworks. The fabrication of a 2-D polymer from chain motifs and additional linking ligands, that is, warp and woof components, has been shown to be quite useful in the construction of tetragonal copper lattices. This

concept can also be applied to a wide variety of compounds having square lattices.

The second interesting point we should consider is flexibility of the sheet to intercalate guest molecules. As far as we concern with our compounds, the guest molecule is primarily different in size. The distances of O−H---N (guest molecules) fall within the range of 2.74−2.80 Å, insensitive to the guest. The interlayer distances of the compounds obtained in this study increase in the order, 8.45 Å (**6**), 9.25 Å (**1b**), 10.24 Å (**1a**), and 11.03 Å (**2**). The interlayer distance is not uniquely determined for an inserted molecule and distribute in some range as is found in polymorphism of dmpyz compounds, **1a** and **1b**. However, degree in lengthening the distance mostly correlates well with the size of a molecule, indicative of stability of 2-D sheet structure and flexibility of the sheet packing. In order to keep this unique structure, both hydrogen bonding and stack-capability of a guest molecule is required. In particular the stack column of guest molecules is important for the stable formation of the sheet structure, otherwise the hydrogen bonding of H_2O and CA for sheet formation is broken by that of the guest molecules as is well illustrated in **7**.

(77) $Cu_2Cl_4O_{12}C_{12}H_8$, $M = 613.09$, monoclinic, space group C_2/c, $a = 17.790(8)$ Å, $b = 7.639(6)$ Å, $c = 10.307(7)$ Å, $\beta = 108.08(4)°$, $V = 1331(1)$ Å^3, $Z = 2$. $R = 0.152$, $R_w = 0.215$. The detailed crystallographic procedure and data are filed in the Supporting Information. Unfortunately, the X-ray data collection was incomplete due to rapid decomposition of the crystal during measurements. However, we could determine an outline-view of the sheet structure (Supporting Figures 1 and 2).

(78) The interlayer distance is defined as that between the nearest-neighbor copper atoms, which belong to the adjacent two sheets, respectively.

We have demonstrated that $[Cu(CA)(H_2O)_2]_k$ chain is a good motif to construct huge structure in the crystal phase and have also demonstrated a pathway to control the crystal structures for Cu/CA/H_2O, guest molecule systems. By coordination or hydrogen bond, the $[Cu(CA)(H_2O)_2]_k$ chain provides the layers, in between which various kinds of guest molecules can be intercalated. The guest molecule used in this work, which is a member of diazene family and has two hydrogen bond sites, takes a key role in controlling crystal structure: (1) coordination bond to link chains (pyz), (2) hydrogen bond to link chains (dmpyz and phz), (3) hydrogen bond to isolate chains (ohphz). The hydrogen bond interaction in (2) and (3) is delicately balanced with the stack interaction and makes the structural chemistry of transition metal−chloranilate compounds fruitful. Therefore it would be possible to create new materials if the hydrogen-bonded sheets, $\{[Cu(CA)(H_2O)_2]_n\}_l$, intercalate various kinds of organic molecules which have potential functions such as conducting and/or photosensitized properties.

Acknowledgment. This research was supported by a Grant-in-Aid for Scientific Research on Priority Area "Molecular Superstructure" (Area No. 262/07241255) from the Ministry of Education, Science, and Culture, Japan, and the Nissan Science Foundation.

Supporting Information Available: Tables providing complete listings of crystallographic data, atomic coordinates, bond lengths, bond angles, anisotropic thermal parameters, for complexes **1a**, **1b**, **2**, **6**, and **7** and a view of **6** and packing diagrams for **6** (29 pages). Ordering information is given on any current masthead page.

IC9603520